scientific reports

OPEN

Miniaturized antenna verified with diffuse optical measurements for native and boiled adipose tissue differentiation

Ashraf S. Abdel Halim[1], Mohanad Mostafa[1] & Omnia Hamdy[2]✉

Medical industries are continuously working towards the development of wearable theragnostic devices which enable monitoring various ailments in the body and then transmitting them to the base-station. The antenna design is of prime importance where the suitable design guarantees proper communication between the antenna and the base-station. In this paper, a co-planar wave-guide antenna is proposed for the use in the medical implant communication service (MICS) band for data transmission. The proposed antenna is studied for ex-vivo applications where the antenna is simulated for bovine intramuscular fat (adipose tissue). The preliminary results showed that the antenna radiates in MICS band. Two types of samples are tested; namely, native fat and boiled fat. The boiled fat is used in order to represent the infected fat tissue. Hence, the antenna was implanted into the fat samples and the results revealed noticeable variations in the radiation characteristics between native and boiled fat. Different parameters of the proposed antenna including the reflection coefficient (S_{11}), radiation patterns, gain, efficiency, and front-to-back ratio are investigated. The simulations showed that S_{11} parameter was − 12.4 dB in MICS band for the normal fat. On the other hand, the measured S_{11} values were − 12.3 dB for the native samples and − 9.9 dB for the boiled fat samples. To assert the variation in the biological characteristics of the boiled fat as compared to those of the native fat, diffuse optical measurements of the examined samples were investigated. Such variation in the light scattering and absorbance by the tissue is responsible for varying the S_{11} parameter for each case. The results have shown that the proposed design is a good candidate for detecting the change in biological tissue.

Biomedical antenna has been developed in 1960s by Medtronic, USA[1] as a battery powered device. Nowadays, antenna in medical applications provides a virtual environment that has the ability to stimulate and monitor the function of various body organs[2]. The antenna wirelessly transfers information about glucose level, body temperature, pH, and cardiac pressure to a certain receiver (e.g., base-stations in medical centers) via links named "bio-telemetry"[3–5]. The design of the antenna depends on the industrial, scientific and medical (ISM) band for medical telemetry operations. Nonetheless, a recent medical implant communication service (MICS) band (402–405 MHz) has been allocated which is regulated by the United States federal communications commission and the European radio communications committee for bi-directional bio-telemetry operations[6].

The MICS band permits low noise propagation through human body that makes it suitable for low power implanted device circuits[7]. The wavelength for free space is 74 cm in the med radio whereas it is around 12 cm in the ISM bands[8]. Accordingly, there is a need to miniaturize the antenna to be implanted inside the human body considering the biocompatibility properties and other related parameters such as gain, SAR, bandwidth, and directivity. Studying the miniaturized antenna and its radiation characteristics has started since decades. The size of the antenna was directly proportional to the radiation power factor, the total efficiency, and the antenna bandwidth[7]. Later on, different miniaturization techniques has been proposed including the use of high permittivity dielectric substrate, lengthening the current flow path on the patch surface, and inserting shorted pins between the ground and the patch plane. The latter results in developing antennas of relatively small effective size[9].

[1]Department of Communication, Faculty of Engineering, Canadian International College (CIC), Cairo, Egypt. [2]Department of Engineering Applications of Lasers, National Institute of Laser Enhanced Sciences, Cairo University, Giza, Egypt. ✉email: omnia@niles.cu.edu.eg

Ref	Antenna dimension (mm³)	Resonant Freq. (GHz)	BW (MHz)	Gain (dBi)	SAR W/Kg	Test tissue
[35]	57	0.402	38.6	− 30.8	289	Minced pork
[38]	$10 \times 10 \times 2.54$	0.402	115	− 7	341	Pork
[39]	$20.5 \times 30 \times 0.05$	0.402	3.73	− 32	513.7	Deep tissue
[40]	$7 \times 6.5 \times 0.377$	0.402	36.8	− 30.5	588	Skin layer
[41]	$22 \times 23 \times 1.27$	0.402	30	− 36.7	832	Skin-mimicking material
[42]	$14 \times 7.5 \times 0.5$	0.405	64	− 40.85	665.35	Scalp (realistic human phantom)
This work	$14 \times 14 \times 0.76$	0.454	0.23	− 10	50	Fat

Table 1. Performance comparison between the proposed antenna and the relevant literature.

Since the signal is highly attenuated within the human body, the near-field effect of antenna causes an increase in the temperature of neighboring tissues. Higher frequency operation also causes similar effect. This may be useful for some therapeutic applications yet shows a negative impact on communication[7]. Utilizing meandered antennas has solved such problem. The meandered structure can miniaturize the size of the antenna and keep the same radiation properties for an implantable antenna[8].

Micro-strip (or patch) antennas have the advantages of being low cost, light weight, compact size and easy fabrication. However, a typical micro-strip antenna has a relatively narrow bandwidth[10]. Therefore, various techniques to enhance the bandwidth of patch antennas have been proposed including substrate-integrated suspended-line technique[11], slotted patch[12,13], adding stubs[14,15], proximity coupled technique[16], and cutting edges[17]. Also, the use of rectangular-shaped coplanar waveguide (CPW) fed printed antennas provides wider bandwidths necessary for wireless and wearable applications[18–21]. Additionally, to increase the gain of the antenna, several advancements are used such as artificial magnetic conductors (AMCs)[22], metamaterials[23] or a horn reflector[24].

Various designs of wireless antennas were developed based on the use of rigid substrates such as FR4 as reported in[25–27]. Nevertheless, for implanting purpose, the design of efficient antennas requires the use of flexible substrates which have the ability to be incorporated with shapes of irregular surfaces[28]. Example of these flexible substrate are kapton[29], liquid crystal polymer (LCP)[30], Rogers RT/duroid[31], cotton layer[32], polyethylene terephthalate (PET) film[33], and paper[34]. A flexible material such as Rogers ULTRALAM has been utilized for multiband conformal implantable antenna fabrication which is utilized in ingestible capsule endoscope and biotelemetry applications[35]. Moreover, antennas can be designed in different shapes including flat and capsule shapes. The capsule antennas are suitable for deep tissue implantation such as intestine, stomach and heart, while the flat type is used for skin (e.g., scalp) implantation[36,37]. Table 1 presents a comparison between the proposed antenna performance and the state-of-the-art designs.

In the present paper, a micro-strip antenna is designed for monitoring adipose tissue (fat) at two different conditions (native and boiled). The antenna is designed in a simple double layered meandered structure. The different antenna parameters are evaluated at each tissue condition. The proposed antenna radiates near the MICS band for data transmission related to patient monitoring. Additionally, diffuse reflectance and transmittance of the examined samples were measured at four laser wavelengths (532, 660, 780 and 980 nm) using integrating sphere-based optical setup to emphasize the difference in tissue properties at each condition, which in turn results in varying the reflection coefficient (S_{11}).

Antenna design

Design process. A compact antenna of dimensions of $0.116\,\lambda_0 \times 0.116\,\lambda_0 \times 0.006\,\lambda_0$ with respect to the resonant frequency is proposed in the current study. The simulations are performed using a commercial simulation software (High-Frequency Structure Simulator Technology (HFSS)). The design is applied on a dielectric substrate Rogers 3210 (dielectric constant = 10.5) to achieve the required characteristics. This substrate has a thickness of 0.76 mm and a loss tangent of 0.0027. It should be noted that the design is primarily based on the meander patch antenna. Figure 1 presents the meander patch antenna. Moreover, the dimensions of the proposed antenna are listed in Table 2.

The first step in the design process is to identify the medium. The proposed antenna is designed to test fat tissue which has dispersive electromagnetic characteristics. The antenna design achieved the 50-Ω excitation in both cases. Figure 2 shows the simulation model in case of fat as a medium. As shown in Fig. 2, the antenna is sandwiched between two layers of fat. The preliminary simulation results for the native fat tissue shows that the resonance frequency achieved by our proposed antenna is 513 MHz.

Design approach. The proposed antenna consists of three layers. The first layer is a ground sheet connected with the patch through the pin. The second layer is the substrate which is divided into two layers that sandwiches the patch (the third layer) between them (see Fig. 3).

The patch layer of the antenna is attached at the top right corner with SMA connector pin. This layer also includes meander tailored resonators and a capacitive coupler gap[43]. The proposed design aims to elongate the current path. The meander structure is bent to decrease the length and increase stiffness of the antenna. A superstrate is usually added to avoid the short circuit between patch and substrate. Therefore, this eliminates the patch to function as a radiating element. Nevertheless, in our proposed design, there is no need to use a
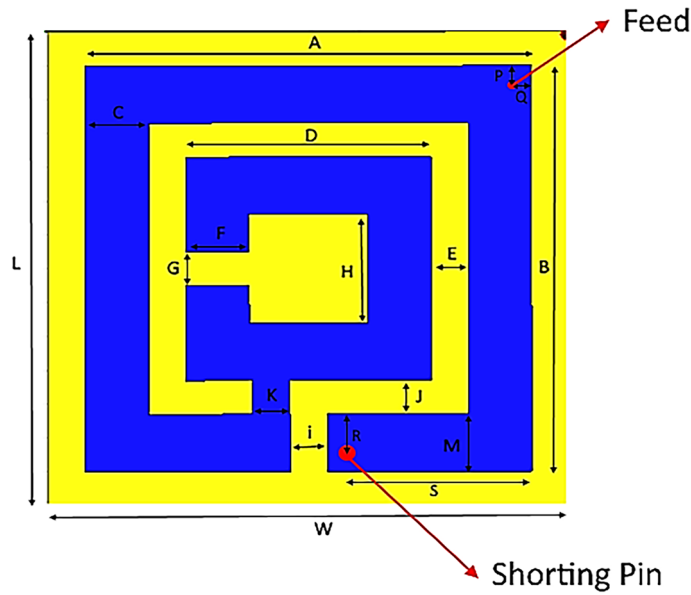
Figure 1. The proposed antenna configuration and dimensions.

A	B	C	D	E	F	G	H	i	J	K	L	M	h	W	P	Q	R	S
12	12	1.7	6.6	1	1.7	1	3.2	1	3.2	1	14	1.7	0.76	14	0.8	0.5	1.2	5

Table 2. Dimensions of the proposed antenna (in mm).
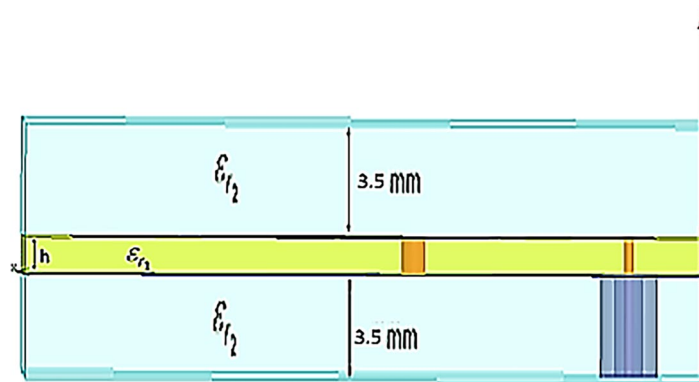
Figure 2. The simulation of the measurement setup in fat.

superstrate due to the poor conductivity of fat material (0.102 S/m). Table 3 represents fat parameters in the resonance frequency. The manufacturing and measurements were performed in the National Telecommunication Institute (NTI), Cairo, Egypt.

Indeed, the microstructural and macroscopic properties of boiled fat are relatively different from the native one[44]. Once the fat is heated, adipose tissue (fat) is liberated from the adipocytes (a cell in connective tissue that is specialized for the fat storage) and its oxidation increases[45]. Accordingly, the electrical conductivity of the fat tissue increases as the temperature increases while decreases if its structure changes[46].

The current distribution. To illustrate the mechanism of operation, the surface current distribution for the proposed antenna is presented in Fig. 4. The current distribution demonstrates that the antenna structure is responsible for producing l dip at 513 MHz as the current concentration along the antenna length. The current concentrates along the antenna width, patch, and pin. The intensive current indicated by red and a null
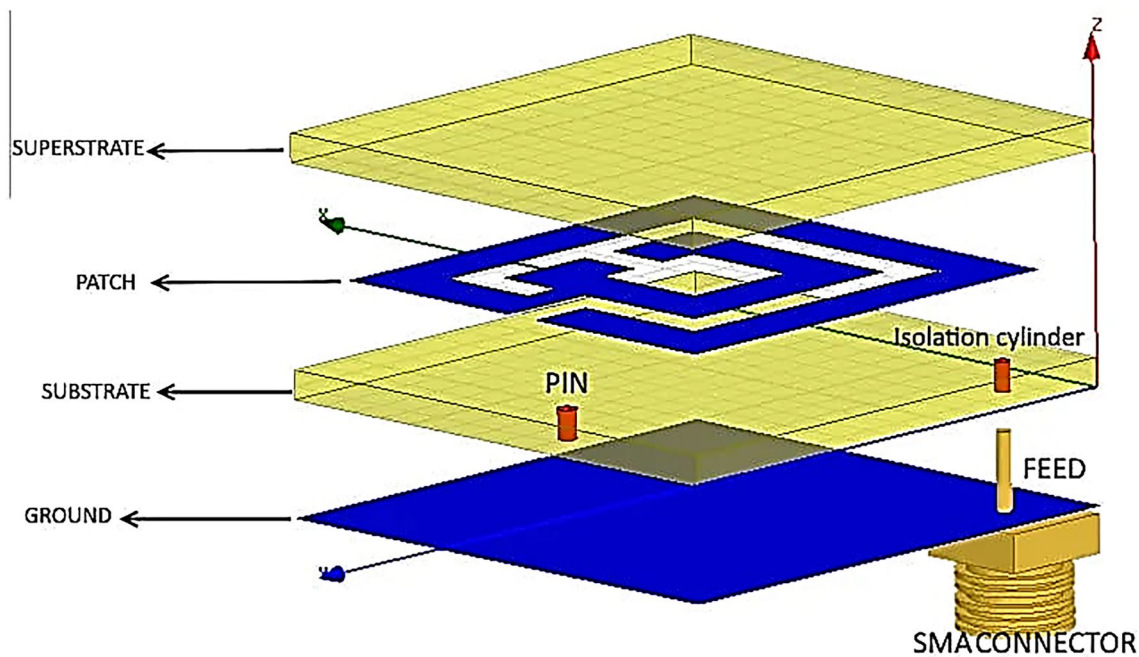
Figure 3. The common design approach of meander antenna.

Tissue	Conductivity	Relative permittivity	Loss tangent	Wavelength	Penetration depth
Fat	0.10235 S/m	5.2853	0.14503	0.054193 m	0.11956 m

Table 3. Fats parameters in the resonance frequency.
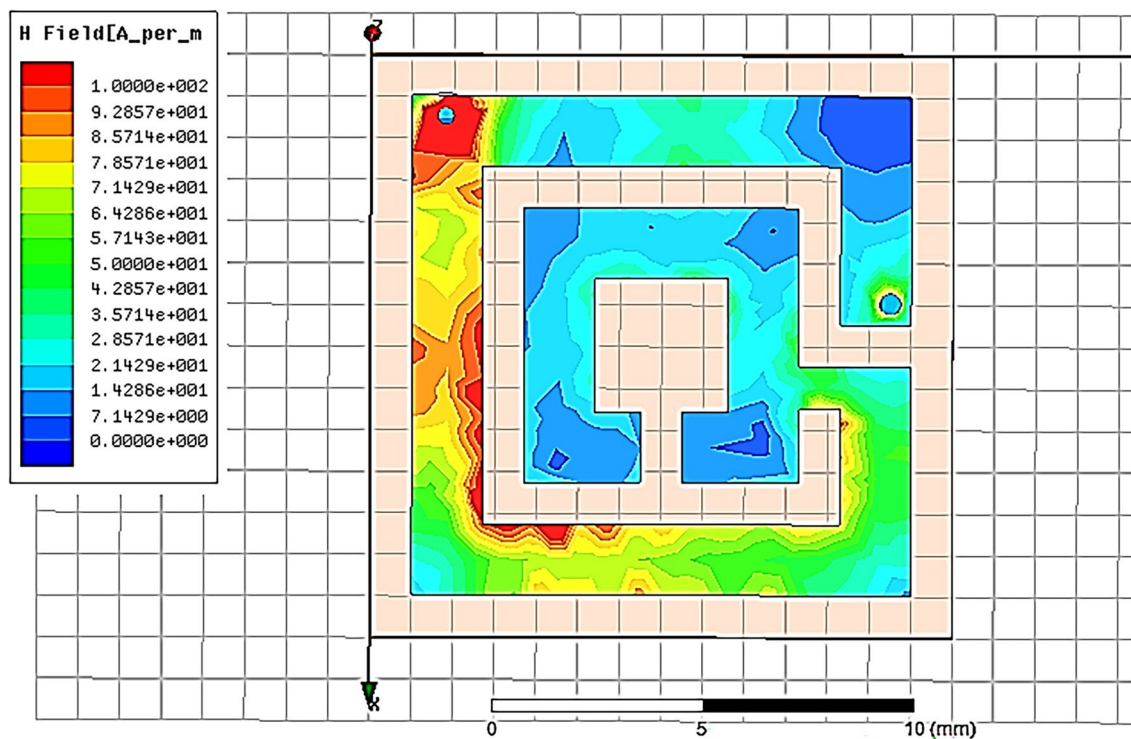
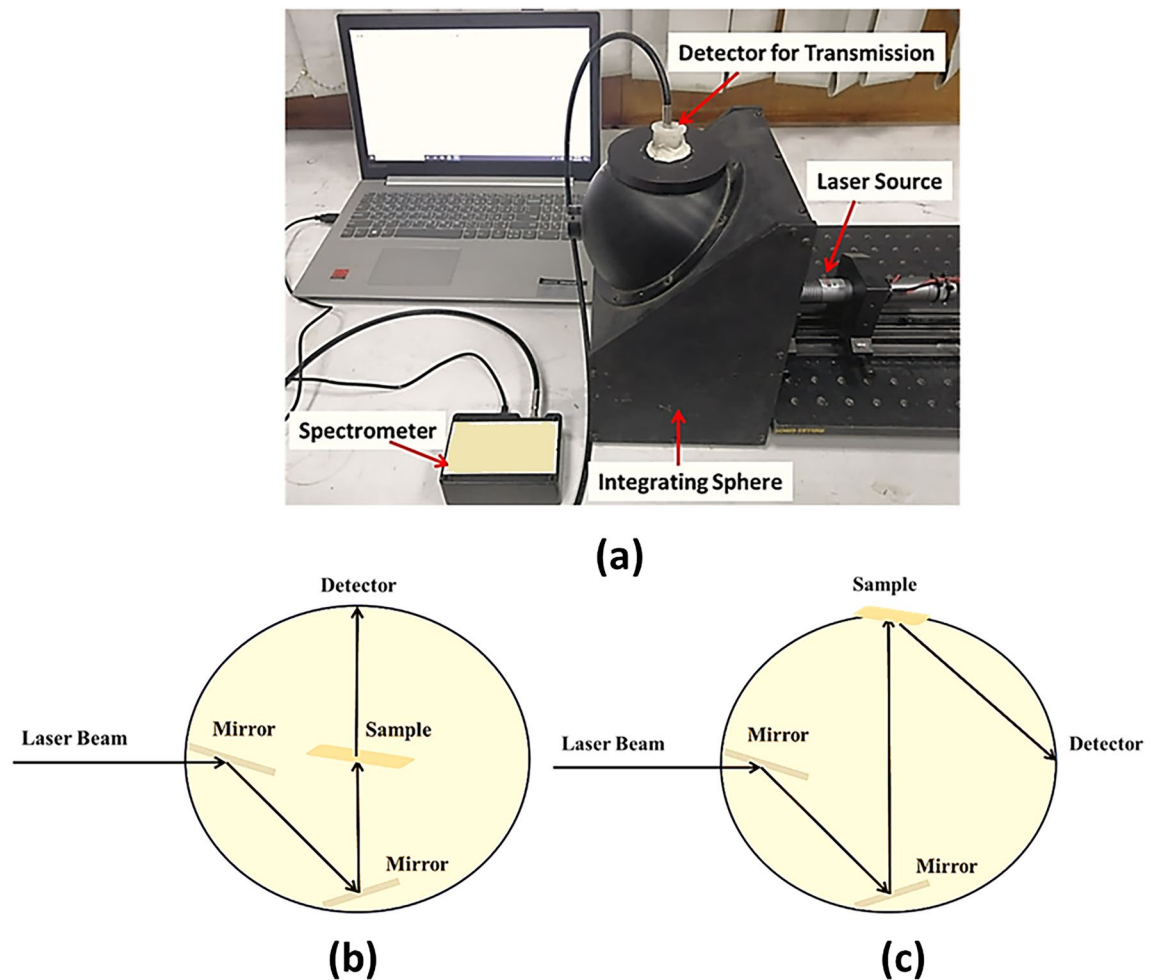**Figure 4.** Current distribution of the proposed antenna at MICS band.

Figure 5. (**a**) The implemented optical setup using integrating sphere, (**b**) schematic of the transmission mode, and (**c**) schematic of the reflection mode.

represented by blue. The figure also illustrates the effective area at which the proposed antenna resonates at the certain frequency.

Diffuse optical measurements

The optical transmission and reflection resulting from light interaction with biological tissue is named as diffuse because of the multiple scattering events affected the light propagation in tissues[47]. The tissue diffuse reflectance/ transmittance is a representative parameter for each tissue, where they vary according to the tissue condition. Therefore, they can be used in tissue differentiation processes[48,49]. Integrating sphere is a very common device that is used for the ex-vivo measurement of the tissue diffuse reflectance and transmittance[50,51]. It is a hollow spherical cavity coated with highly reflective material to ensure reflection of the whole entering light. In our experiments, Barium sulfate coated mcPHERSON integrating sphere has been used to measure diffuse reflectance/transmittance of the native and boiled fat samples. A photo of the experimental setup is presented in Fig. 5a.

A typical integrating sphere has multiple ports and locations for placing the sample under investigation. Furthermore, a light detector is used where its location is dependent on the required measurement (tissue transmittance or reflectance) as demonstrated in Fig. 5b,c, respectively. The tissue's detected diffuse light is then delivered to a compact spectrometer that is connected to a computer for data analysis and processing. In the present work, a digital fiber spectrometer (STDFSM, Touptek Photonics Co. Ltd, Zhejiang China) integrated with a detector (Toshiba TCD1304AP linear CCD array) has been used.

Collecting fat samples. Ex-vivo bovine intramuscular fat (adipose tissue) samples have been collected from different butcher shops. There is no direct contact with alive animals in the present study. Therefore, no specific ethical approval is required. The sources of the utilized fat samples (bovines) were already slaughtered for commercial food production and the fat tissues can be considered as disposals or remains.
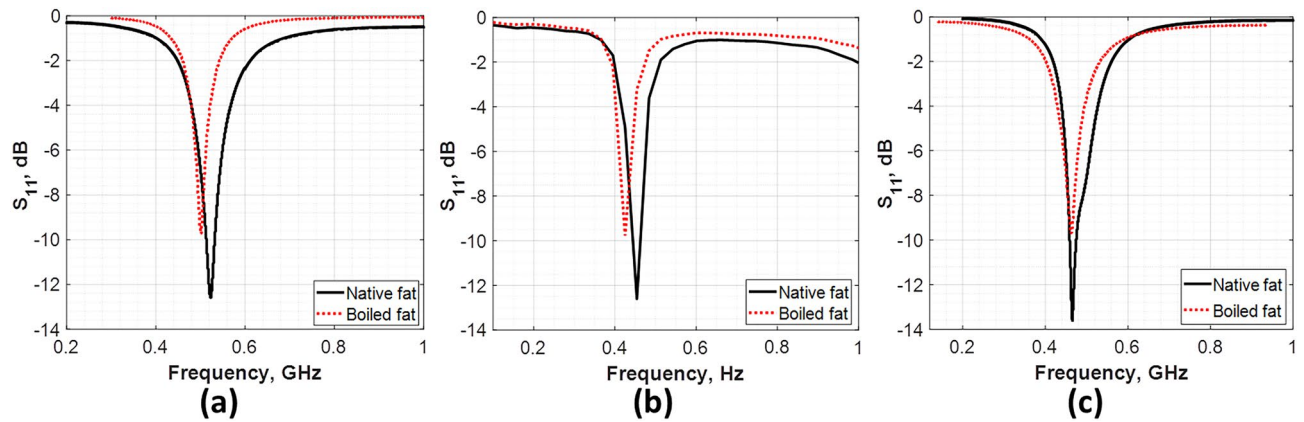
Figure 6. The measured reflection coefficient (S11) of the three fabricated antennas for native and boiled fat tissues.

Results and discussion

To evaluate the proposed design, a Rohde&Schwarz ZVB 20 (Vector Network Analyzer, 10 MHz–20 GHz) is used to test the antenna. As previously mentioned, the fat is examined in this study in two cases; normal and infected (the infected was represented by the boiled tissue). For better profess, three similar antennas with the same design and material were fabricated and measured. Figure 6 shows the measured reflection coefficient of each antenna at the two examined tissue conditions.

Photographs of the fabricated antennas before and after immersed in the fat sample is presented in Fig. 7a,b respectively. Moreover, a comparison between the simulated and average measured reflection coefficient (S_{11}) for the three antennas is presented in Fig. 7c.

Figure 7c illustrates the S_{11} parameter for the three cases; simulations, native tissue and infected tissue (boiled). In the simulations, S_{11} was − 12.4 dB at 0.513 GHz. However, in the case of native fat the S_{11} was − 12.3 dB. In case of infected fat S_{11} changed to − 9.9 dB. In the measurements, both native and infected fat exhibit a frequency shift to the left with respect to that of the simulated value (i.e., 0.454 GHz for the native fat and 0.425 GHz for the infected fat). The observed frequency shift in the three cases is attributed to the non-uniform thickness (structure) of the examined fat tissue samples at the different conditions (native and boiled samples). In addition, the possible fabrication tolerance may lead to the same effect. Table 4 summarizes the results of the proposed antenna.

The radiation patterns. The E-plane of the radiation pattern of the proposed antenna (E_θ at $\varphi = 0°$) and the H-plane radiation pattern (E_θ at $\varphi = 90°$) is presented in Fig. 8.

The E-plane radiation patterns show that the proposed antenna radiates omnidirectional in case of simulated and boiled tissue and bi-directional in case of normal fat. However, the H-plane patterns reveal that the antenna radiates bi-directional in the three cases. It is worth noting that the model does not take into account the probe location. It is also assumes that the dielectric material of the substrate is truncated and does not cover the ground plane beyond the edges of the patch which may be the cause of the discrepancies between the two patterns.

The 3-D radiation patterns for the proposed antenna at the resonance frequency for the three configurations; simulated, normal and boiled fat are illustrated in Fig. 9a–c, respectively.

The gain. Figure 10 shows the gain of the proposed antenna. The maximum obtained gain in the MICS band was about − 10 dB. This is due to limitations in the measurement process in addition to the degenerative effect of the SMA connector due to small size of the antenna.

SAR. The electromagnetic parameters of the human tissue are given in Table 5. The calculation formula of SAR value is presented as follows:

$$SAR = \frac{\sigma E^2}{\rho} \tag{1}$$

where σ is conductivity, E is the electric field intensity, and ρ is the mass density[52].

The average SAR value of the proposed antenna when implanted into the fat tissue is presented in Fig. 11. The maximum SAR of the 10 g is 50 W/Kg. Due to the reflection characteristics, the obtained SAR enhances the main lobe but it also reduces the back lobe. This means that only a small amount of electromagnetic wave energy is radiated to the fat tissue. Therefore, the antenna has good forward radiation and reasonable SAR value.

Total efficiency and front to back ratio. The simulated total efficiency and front to back ratio "FBR" versus frequency of the proposed antenna are presented in Fig. 12a,b, respectively.

As shown in Fig. 12a, the total efficiency of the antenna is almost − 10 dB at the operational frequency. In addition, a relatively high FBR is obtained at the resonance frequency of the antenna (see Fig. 12b).
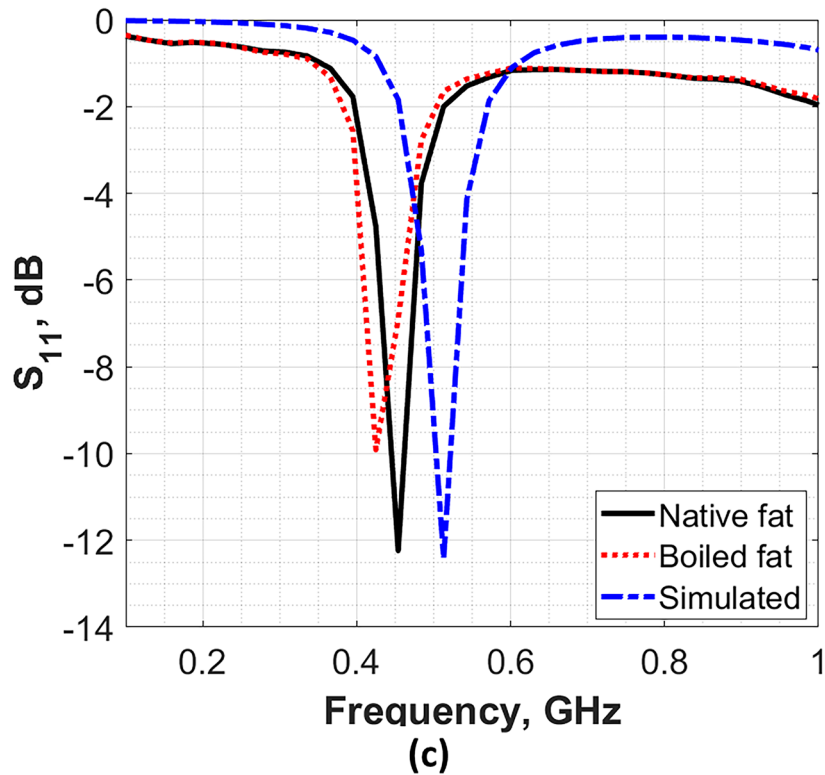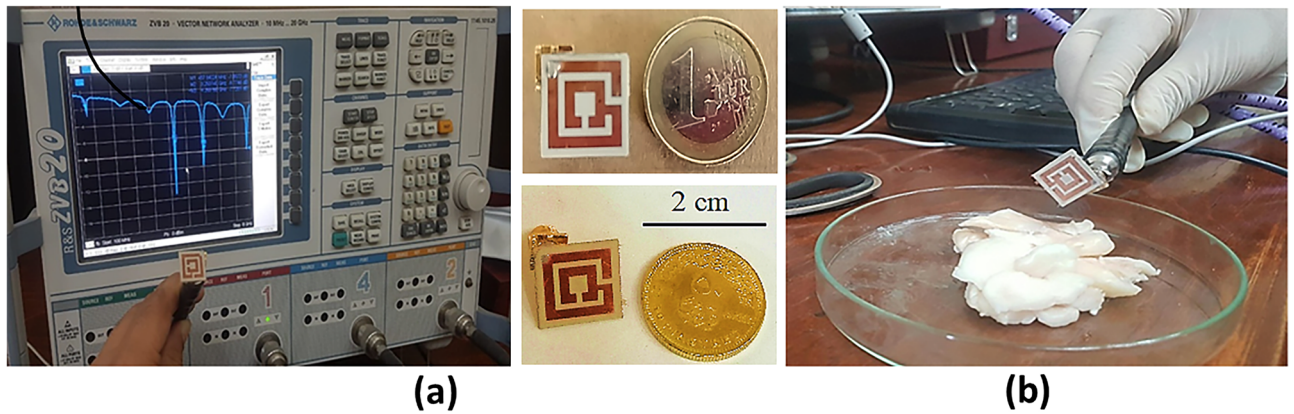
Figure 7. (**a**) A photograph of the fabricated antennas, (**b**) a photograph of the antenna with studied fat sample, (**c**) the S$_{11}$ parameters for simulation, normal and boiled fat.

	Validation	Operating frequency (GHz)	Reflection coefficient, S11 (dB)	−3- dB Bandwidth (MHz)
Simulated	Native fat	0.513	− 12.4	0.20
Measured	Native fat	0.454	− 12.3 ± 0.3	0.19 ± 0.02
	Boiled fat	0.425	− 9.9 ± 0.2	0.17 ± 0.01

Table 4. Summary of the simulated and measured antenna results.

Diffuse optical measurements. Tissue reflectance is the ratio between the reflected light intensity and the incident light intensity, while the transmittance is defined as the ratio between the transmitted light intensity and the incident light intensity. Accordingly, the variations in the reflected light intensity and transmitted light intensity of the fat samples (native and boiled) at each wavelength are presented in Figs. 13 and 14, respectively. For each sample, the experimental measurements have been obtained five times and the average values are plotted.

As shown in Fig. 13, the diffuse reflectance of the boiled fat tissues is less than the native tissues at the four studied wavelengths. On the other hand, the transmittance measurements show the opposite behavior (Fig. 14).
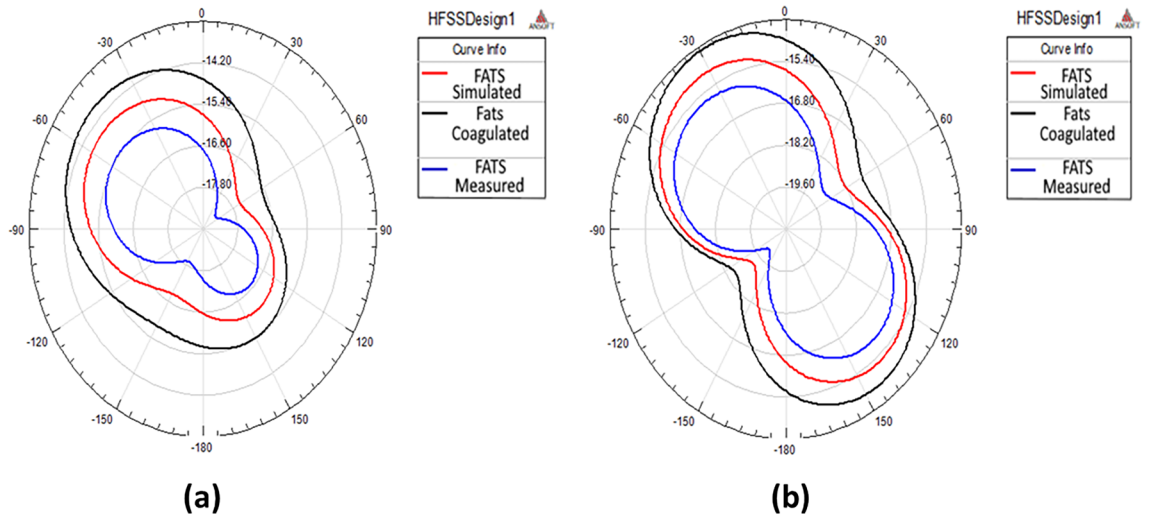
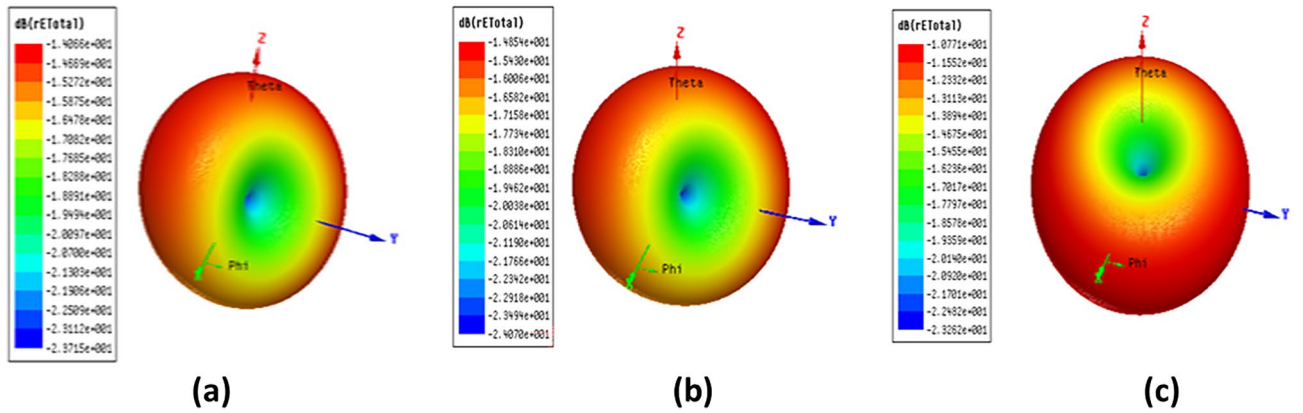**Figure 8.** The Radiation pattern (**a**) E-plane at $\varphi = 0$ and (**b**) H-plane at $\varphi = 90°$.

Figure 9. The 3-D radiation patterns for the proposed antenna (**a**) simulation, (**b**) normal fat and (**c**) boiled fat.
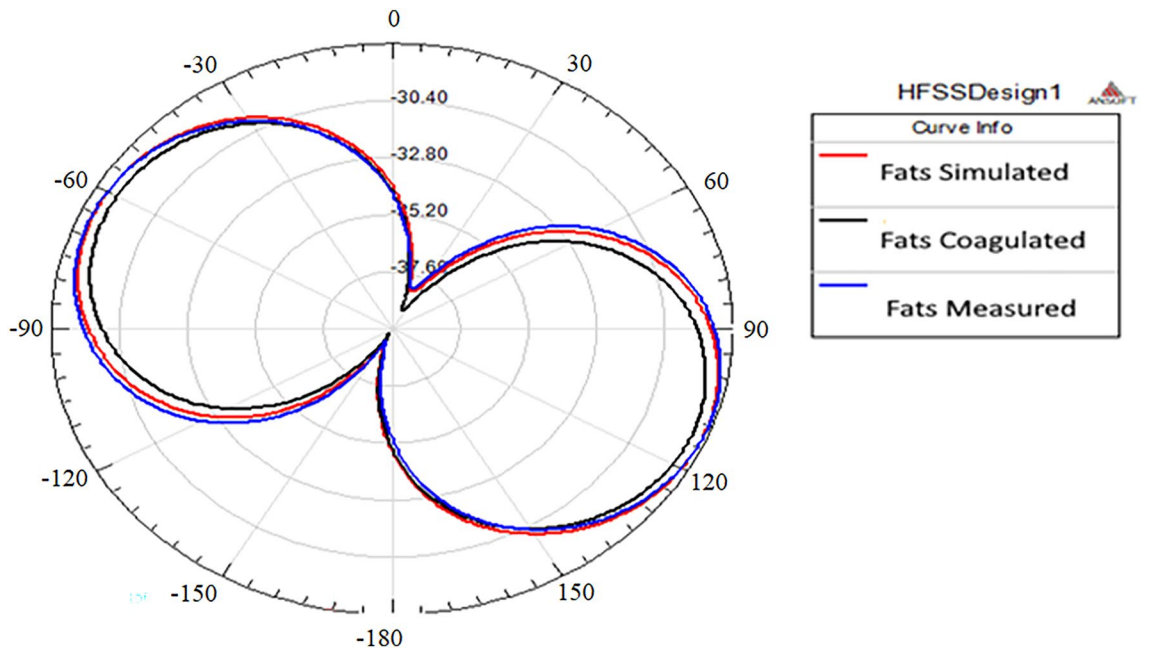

Figure 10. The gain of the proposed antenna.

Tissue	ε_r	Conductivity (S/m)	Density (kg/m³)	Thickness (mm)
Skin	37.95	1.49	1001	2
Fat	5.27	0.10235	900	5
Muscle	52.67	1.77	1006	20
Bone	18.49	0.82	1008	13

Table 5. The electromagnetic parameters of the human tissue.
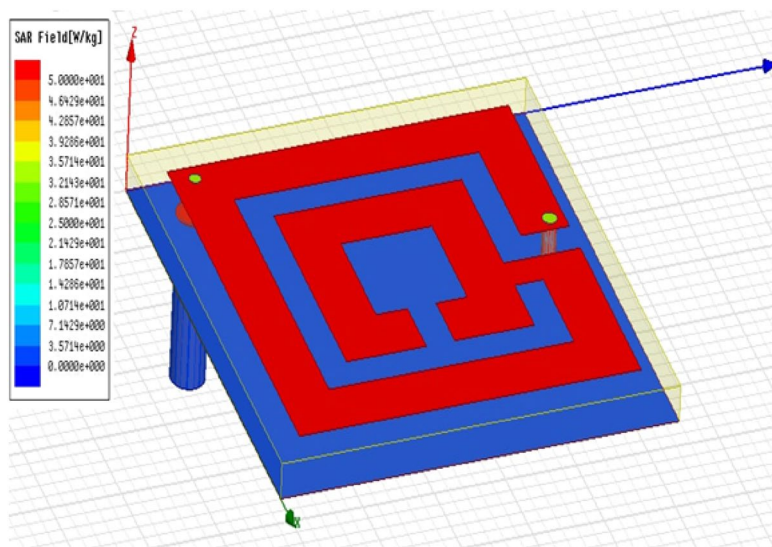
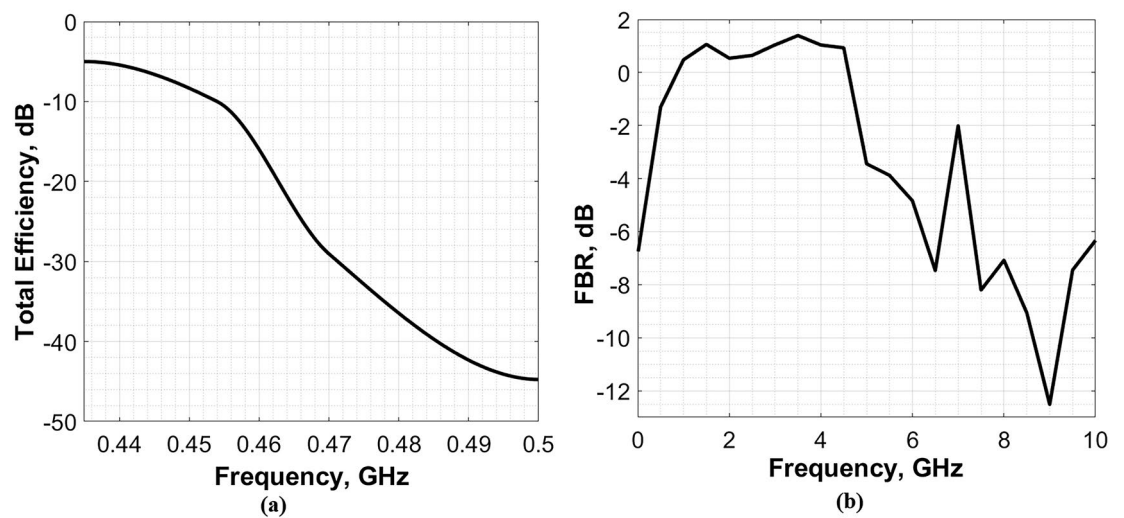**Figure 11.** Simulated SAR of the proposed antenna.

Figure 12. The simulated (**a**) total efficiency, and (**b**) front to back ratio of the proposed antenna.
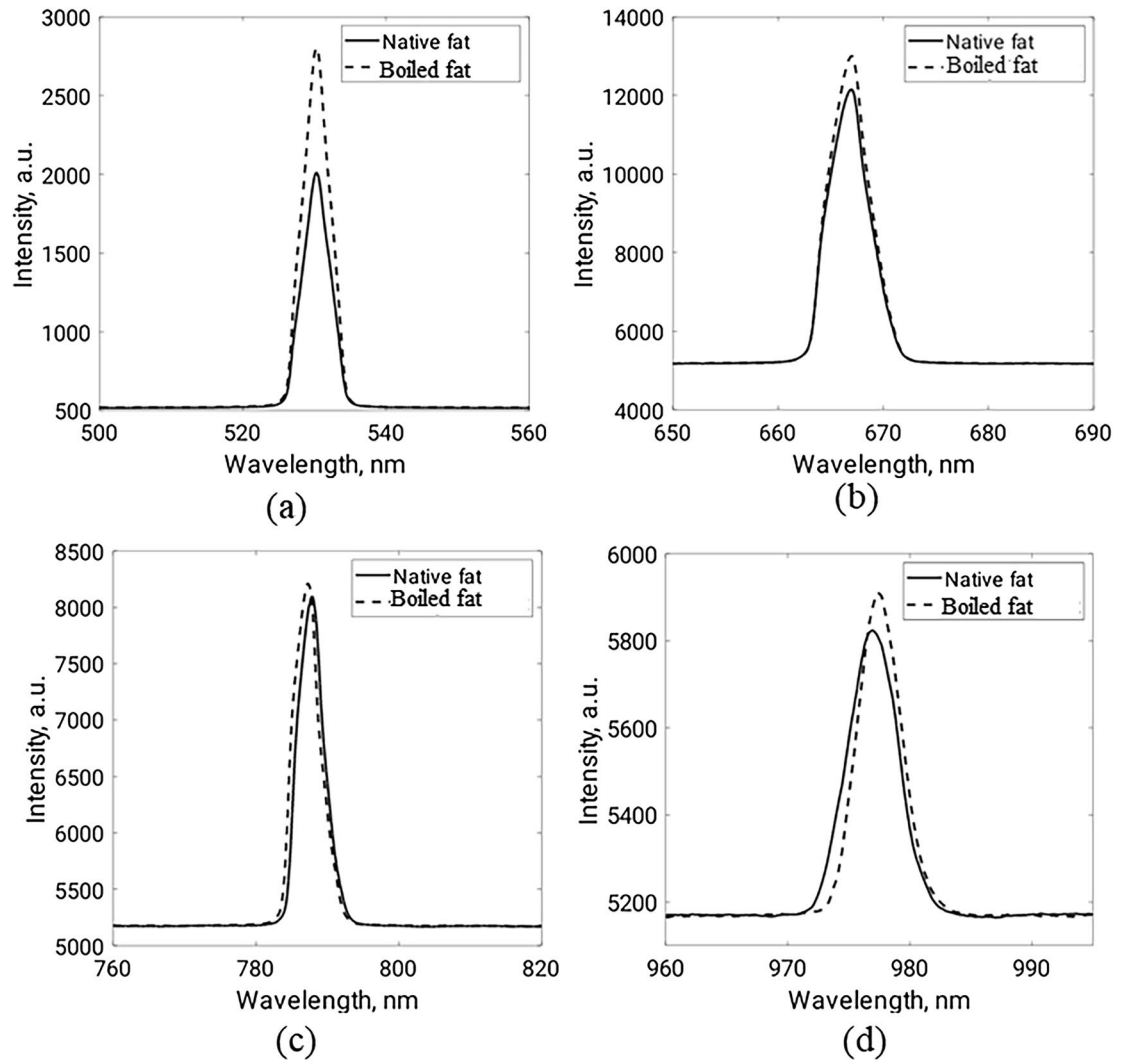
Figure 13. Diffuse reflected light of fat samples at (**a**) 532 nm, (**b**) 660 nm, (**c**) 780 nm, and (**d**) 980 nm.

Such results are reasonable as some cellular and intracellular characteristics (such as protein denaturation, hyalinization of collagen, and cell membrane rupture) of fat tissues are supposed to be altered after boiling[53]. These characteristics have a great effect on tissue scattering properties and hence affect light distribution and propagation[54].

Conclusions

A miniaturized multilayer antenna was designed as a diagnostic tool for differentiating native and infected adipose tissue (ex-vivo bovine fat). An additional substrate was added to the design to enable the antenna to test high conductive tissues. The antenna resonated at 454 MHz (near to the MICS band), which makes it applicable for the short range medical applications. Although the resonant frequency of the proposed antenna does not lay exactly in the MICS band (402–405 MHz), the measured reflection coefficient (S_{11}) showed a considerable change at the different conditions of the tissue. Additionally, the measured results of the proposed antenna showed an acceptable agreement with the simulation results. Moreover, the E- and H-field radiation patterns asserted the same conclusions. The antenna gain was − 10 dB in the three cases. Furthermore, the diffuse reflectance and transmittance of the studied tissue samples were measured to confirm the variation in the optical properties between native and infected samples which was also demonstrated in the obtained S_{11} parameter at each case. Compared with the previous literature, the proposed antenna has relatively small dimensions. For future investigations, the proposed antenna will be tested on other tissues with high conductivity. Additionally, multiple antennas with different designs using various Rogers will be considered.
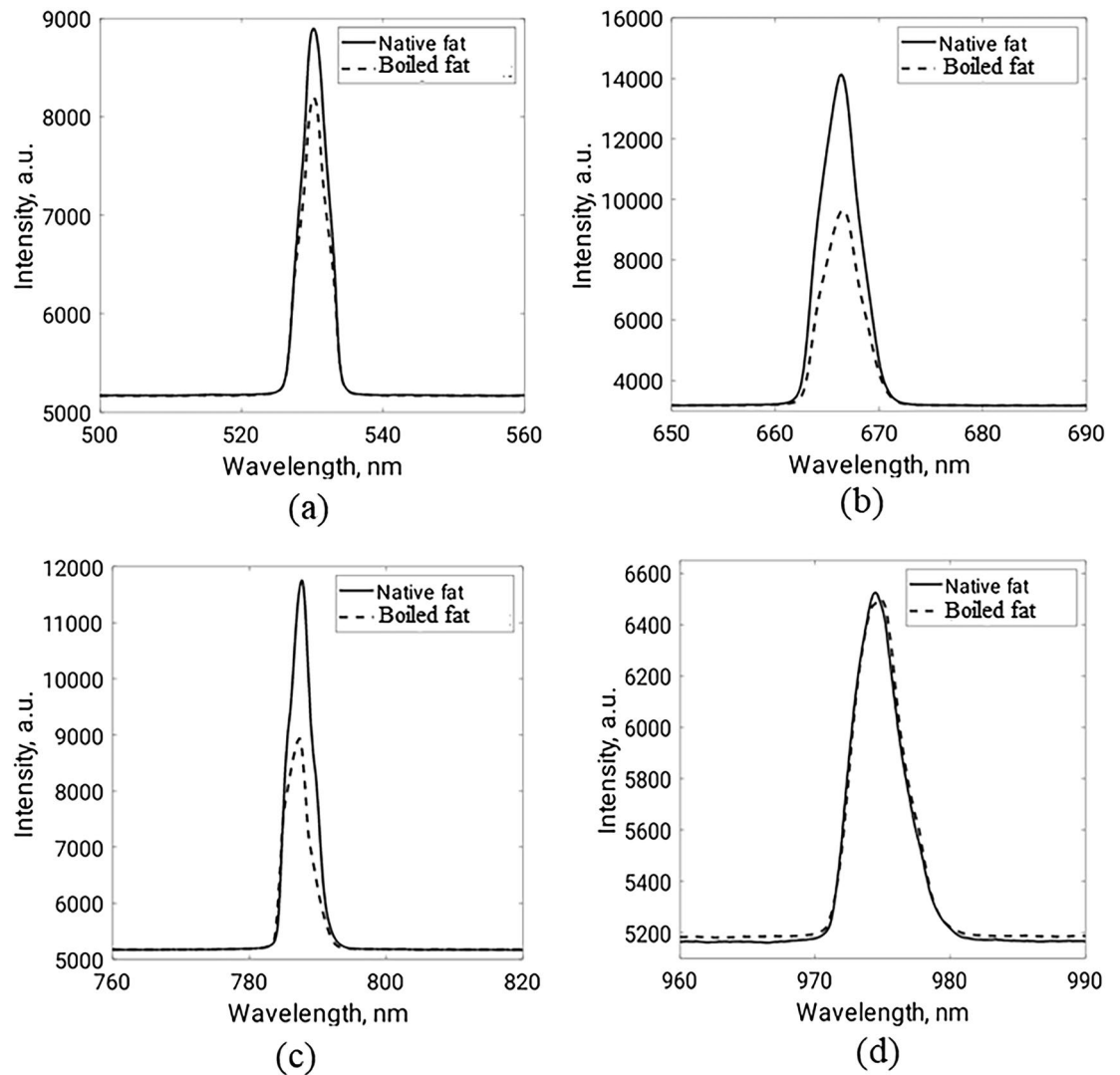
Figure 14. Total transmitted light of fat samples at (**a**) 532 nm, (**b**) 660 nm, (**c**) 780 nm, and (**d**) 980 nm.

Data availability
The datasets used and/or analyzed during the current study available from the corresponding author on reasonable request.

References
1. Bhattacharjee, S., Maity, S., Metya, S. K. & Bhunia, C. T. Performance enhancement of implantable medical antenna using differential feed technique. *Eng. Sci. Technol. Int. J.* **19**, 642–650 (2016).
2. Cosoli, G., Scalise, L., Poli, A. & Spinsante, S. Wearable devices as a valid support for diagnostic excellence: lessons from a pandemic going forward. *Health Technol. (Berl)* **11**, 673–675 (2021).
3. Taylor, W. *et al.* A review of the state of the art in non-contact sensing for covid-19. *Sensors* **20**, 1–19 (2020).
4. Yun, S. M. *et al.* Recent advances in wearable devices for non-invasive sensing. *Appl. Sci.* **11**, 1–28 (2021).
5. Liao, Y., Leeson, M. S. & Higgins, M. D. A communication link analysis based on biological implant wireless body area networks. *Appl. Comput. Electromagn. Soc. J.* **31**, 619–628 (2016).
6. Kiourti, A., Costa, J. R., Fernandes, C. A., Santiago, A. G. & Nikita, K. S. Miniature implantable antennas for biomedical telemetry: From simulation to realization. *IEEE Trans. Biomed. Eng.* **59**, 3140–3147 (2012).
7. Kiourti, A., Costa, J. R., Fernandes, C. A. & Nikita, K. S. A broadband implantable and a dual-band on-body repeater antenna: Design and transmission performance. *IEEE Trans. Antennas Propag.* **62**, 2899–2908 (2014).
8. Skrivervik, A. K. Implantable antennas: The challenge of efficiency. in *7th European Conference on Antennas and Propagation (EuCAP)* 3627–3631 (2013).
9. Kiourti, A. & Nikita, K. S. A review of implantable patch antennas for biomedical telemetry: Challenges and solutions. *IEEE Antennas Propag. Mag.* **54**, 210–228 (2012).
10. Liu, Y. *et al.* Some recent developments of microstrip antenna. *Int. J. Antennas Propag.* https://doi.org/10.1155/2012/428284 (2012).
11. He, Y., Ma, K., Yan, N. & Zhang, H. Dual-band monopole antenna using substrate-integrated suspended line technology for WLAN application. *IEEE Antennas Wirel. Propag. Lett.* **16**, 2776–2779 (2017).

12. Boukarkar, A., Lin, X. Q., Jiang, Y. & Yu, Y. Q. Miniaturized Single-Feed Multiband Patch Antennas. *IEEE Trans. Antennas Propag.* **65**, 850–854 (2017).
13. Araghi, A. A compact planar ultra wideband antenna with triple-notched bands using capacitive coupled and parallel LC elements. *Appl. Comput. Electromagn. Soc. J.* **31**, 1416–1420 (2016).
14. Cao, Y. F., Cheung, S. W. & Yuk, T. I. A multiband slot antenna for GPS/WiMAX/WLAN systems. *IEEE Trans. Antennas Propag.* **63**, 952–958 (2015).
15. Gad, N. H. & Vidmar, M. Design of a Microstrip-fed printed-slot antenna using defected ground structures for Multiband applications. *Appl. Comput. Electromagn. Soc. J.* **33**, 854–860 (2018).
16. Majidi, N. *et al.* Design and comparison of 4 types of dual resonance proximity coupled microstrip patch antennas. *Appl. Comput. Electromagn. Soc. J.* **33**, 1135–1139 (2018).
17. Hsu, C. K. & Chung, S. J. Compact multiband antenna for handsets with a conducting edge. *IEEE Trans. Antennas Propag.* **63**, 5102–5107 (2015).
18. Prabakaran, N. *et al.* A coplanar waveguide (CPW) fed circular microstripantenna for UWB applications. *Int. J. Innov. Technol. Explor. Eng.* **8**, 531–534 (2019).
19. Shanmuganantham, T., Balamanikandan, K. & Raghavan, S. CPW-fed slot antenna for wideband applications. *Int. J. Antennas Propag.* 1–4 (2008). https://doi.org/10.1155/2008/379247.
20. Kadry, M., Atrash, M. El & Abdalla, M. A. Design of an ultra-thin compact flexible dual-band antenna for wearable applications. in *2018 IEEE International Symposium on Antennas and Propagation & USNC/URSI National Radio Science Meeting* 1949–1950 (2018). https://doi.org/10.1109/APUSNCURSINRSM.2018.8609247.
21. Abdalgalil, O. F., Atrash, M. El & Abdalla, M. A. a flexible high gain wide-band antenna for wireless and wearable applications. in *2018 IEEE International Symposium on Antennas and Propagation & USNC/URSI National Radio Science Meeting* 1279–1280 (2018). https://doi.org/10.1109/APUSNCURSINRSM.2018.8608830.
22. Bean, D. & Venkataraman, J. Gain Enhancement of on-chip antenna at 60 GHz using an artificial magnetic conductor. in *2020 IEEE International Symposium on Antennas and Propagation and North American Radio Science Meeting* 1423–1424 (2020).
23. Pandit, S., Mohan, A. & Ray, P. A low-profile high-gain substrate-integrated waveguide-slot antenna with suppressed cross polarization using metamaterial. *IEEE Antennas Wirel. Propag. Lett.* **16**, 1614–1617 (2017).
24. Ge, Y., Sun, Z., Chen, Z. & Chen, Y. Y. A high-gain wideband low-profile fabry-perot resonator antenna with a conical short horn. *IEEE Antennas Wirel. Propag. Lett.* **15**, 1889–1892 (2016).
25. Wu, M. T. & Chuang, M. L. Multibroadband slotted bow-tie monopole antenna. *IEEE Antennas Wirel. Propag. Lett.* **14**, 887–890 (2015).
26. Supriya, A. S. & Rajendran, J. A low cost tri-band microstrip patch antenna for GPS application. *Prog. Electromagn. Res. Symp.* 60–65 (2017). https://doi.org/10.1109/PIERS-FALL.2017.8293111.
27. Ahmad, A., Arshad, F., Naqvi, S. I., Amin, Y. & Tenhunen, H. Design, fabrication, and measurements of extended l-shaped multiband antenna for wireless applications. *Appl. Comput. Electromagn. Soc. J.* **33**, 388–393 (2018).
28. Kavitha, A. & Swaminathan, J. N. Design of flexible textile antenna using FR4, jeans cotton and teflon substrates. *Microsyst. Technol.* **25**, 1311–1320 (2019).
29. Ahmed, S., Tahir, F. A., Shamim, A. & Cheema, H. M. A compact kapton-based inkjet-printed multiband antenna for flexible wireless devices. *IEEE Antennas Wirel. Propag. Lett.* **14**, 1802–1805 (2015).
30. Haque, E., Mahmuda, S. & Ahmed, F. A capsule-like flexible multiband antenna for WBAN applications. *IEEE Reg. 10 Annu. Int. Conf. Proceedings/TENCON* 1614–1619 (2017). https://doi.org/10.1109/TENCON.2017.8228116.
31. Liu, H. *et al.* Quad-band CPW-fed monopole antenna based on flexible pentangle-loop radiator. *IEEE Antennas Wirel. Propag. Lett.* **14**, 1373–1377 (2015).
32. Hosseini Varkiani, S. M. & Afsahi, M. Grounded CPW multi-band wearable antenna for MBAN and WLAN applications. *Microw. Opt. Technol. Lett.* **60**, 561–568 (2018).
33. Castro, A. T. & Sharma, S. K. Inkjet-printed wideband circularly polarized microstrip patch array antenna on a PET film flexible substrate material. *IEEE Antennas Wirel. Propag. Lett.* **17**, 176–179 (2018).
34. Abutarboush, H. F., Farooqui, M. F. & Shamim, A. Inkjet-printed wideband antenna on resin-coated paper substrate for curved wireless devices. *IEEE Antennas Wirel. Propag. Lett.* **15**, 20–23 (2016).
35. Yousaf, M. *et al.* Compacted conformal implantable antenna with multitasking capabilities for ingestible capsule endoscope. *IEEE Access* **8**, 157617–157627 (2020).
36. Zada, M. & Yoo, H. A miniaturized triple-band implantable antenna system for bio-telemetry applications. *IEEE Trans. Antennas Propag.* **66**, 7378–7382 (2018).
37. Zada, M., Shah, I. A., Basir, A. & Yoo, H. Ultra-compact implantable antenna with enhanced performance for leadless cardiac pacemaker system. *IEEE Trans. Antennas Propag.* **69**, 1152–1157 (2021).
38. Huang, F. J. *et al.* Rectenna application of miniaturized implantable antenna design for triple-band biotelemetry communication. *IEEE Trans. Antennas Propag.* **59**, 2646–2653 (2011).
39. Das, R. & Yoo, H. Biotelemetry and wireless powering for leadless pacemaker systems. *IEEE Microw. Wirel. Components Lett.* **25**, 262–264 (2015).
40. Shah, I. A., Zada, M. & Yoo, H. Design and analysis of a compact-sized multi-band spiral-shaped implantable antenna for scalp implantable and leadless pacemaker systems. *IEEE Trans. Antennas Propag.* **67**, 4230–4234 (2019).
41. Liu, Y., Chen, Y., Lin, H. & Juwono, F. H. A novel differentially fed compact dual-band implantable antenna for biotelemetry applications. *IEEE Antennas Wirel. Propag. Lett.* **15**, 1791–1794 (2016).
42. Gani, I. & Yoo, H. Multi-band antenna system for skin implant. *IEEE Microw. Wirel. Components Lett.* **26**, 294–296 (2016).
43. Abbasi, M. A. B., Shahid, S., Rizwan, M., Tarar, M. A. & Abbas, S. M. On-board printed handset antenna with coupled monopoles. *8th Eur. Conf. Antennas Propagation, EuCAP 2014* 2889–2892 (2014). https://doi.org/10.1109/EuCAP.2014.6902430.
44. Glorieux, S. *et al.* Effect of meat type, animal fat type, and cooking temperature on microstructural and macroscopic properties of cooked sausages. *Food Bioprocess Technol.* **12**, 16–26 (2019).
45. El-Zayat, S. R., Sibaii, H. & El-Shamy, K. A. Physiological effects of fat loss. *Bull. Natl. Res. Cent.* **43**, 1–15 (2019).
46. Bozkurt, H. & Icier, F. Electrical conductivity changes of minced beef-fat blends during ohmic cooking. *J. Food Eng.* **96**, 86–92 (2010).
47. Wang, L. V., Wu, H. *Biomedical Optics: Principles and Imaging.* (Wiley-Interscience, 2007).
48. Hamdy, O. & Mohammed, H. S. Investigating the transmission profiles of 808 nm laser through different regions of the rat's head. *Lasers Med. Sci.* **36**, 803–810 (2021).
49. Hamdy, O., Fathy, M., Al-Saeed, T. A., El-Azab, J. & Solouma, N. H. Estimation of optical parameters and fluence rate distribution in biological tissues via a single integrating sphere optical setup. *Optik (Stuttg).* **140**, 1004–1009 (2017).
50. Hamdy, O. & Solouma, N. H. Distant-detector versus integrating sphere measurements for estimating tissue optical parameters: A comparative experimental study. *Optik (Stuttg).* **247**, 167981 (2021).
51. Hamdy, O. & Mohammed, H. S. Variations in tissue optical parameters with the incident power of an infrared laser. *PLoS ONE* **17**, e0263164 (2022).
52. Saeed, S. M., Balanis, C. A., Birtcher, C. R., Durgun, A. C. & Shaman, H. N. Wearable flexible reconfigurable antenna integrated with artificial magnetic conductor. *IEEE Antennas Wirel. Propag. Lett.* **16**, 2396–2399 (2017).

53. Larin, K. V., Larina, I. V. & Esenaliev, R. O. Monitoring of tissue coagulation during thermotherapy using optoacoustic technique. *J. Phys. D. Appl. Phys.* **38**, 2645–2653 (2005).
54. Hamdy, O., El-Azab, J., Al-Saeed, T. A., Hassan, M. F. & Solouma, N. H. A method for medical diagnosis based on optical fluence rate distribution at tissue surface. *Materials (Basel).* **10**, 1–13 (2017).

Acknowledgements

Author contributions

Study design and conceptualization: A.S.A.H. and O.H. Writing original draft: O.H. and A.S.A.H. Analyzing results: M.M., A.S.A.H., and O.H. All authors reviewed the final manuscript.

Funding

Competing interests

The authors declare no competing interests.

Additional information

Correspondence and requests for materials should be addressed to O.H.

Reprints and permissions information is available at www.nature.com/reprints.

Publisher's note Springer Nature remains neutral with regard to jurisdictional claims in published maps and institutional affiliations.